Ⓔ

THE DETECTABILITY OF ORPHAN AFTERGLOWS

EHUD NAKAR AND TSVI PIRAN

Racah Institute for Physics, The Hebrew University, Jerusalem 91904, Israel

AND

JONATHAN GRANOT

Institute for Advanced Studies, Princeton, NJ 08540

ABSTRACT

The realization that gamma-ray bursts (GRBs) release a constant amount of energy implies that post–jet-break afterglow evolution is largely universal. For a given redshift, all afterglows should be detected up to a fixed observer angle. We estimate the observed magnitude and the implied detectability of orphan afterglows. We show that for reasonable limiting magnitudes ($m_{\rm lim} = 25$), orphan afterglows will typically be detected from small ($\sim 10°$) angles away from the GRB jet axis. A detected orphan afterglow generally corresponds to a " near miss " of a GRB whose jet is pointing just slightly away from us. With our most optimistic parameters, we expect that 15 orphan afterglows will be recorded in the Sloan Digital Sky Survey, and 35 transients will be recorded in a dedicated 2 m class telescope operating full time for a year in an orphan afterglow search. The rate is smaller by a factor of 15 for our " canonical " parameters. We show that for a given facility, an optimal survey should be shallower, covering a larger area, rather than deeper. The limiting magnitude should not be, however, lower than ~ 23, as in this case, more transients from on-axis GRBs will be discovered than orphan afterglows. About 15% of the transients could be discovered with a second exposure of the same area provided that it follows after 3, 4, and 8 days for $m_{\rm lim} = 23$, 25, and 27, respectively.

Subject heading: gamma rays: bursts

On-line material: color figures

1. INTRODUCTION

The realization that gamma-ray bursts (GRBs) are beamed with rather narrow opening angles, while the following afterglow can be observed over a wider angular range, led immediately to the search for orphan afterglows: afterglows that are not associated with observed prompt GRB emission. Rhoads (1997) was the first to suggest that observations of orphan afterglows would enable us to estimate the opening angles and the true rate of GRBs. An expanding jet with an opening angle of θ_j behaves, as long as its Lorentz factor $\gamma > \theta_j^{-1}$, as if it is a part of a spherical shell (Piran 1994). As it slows down and reaches $\gamma \approx \theta_j^{-1}$, the jet quickly expands laterally (Rhoads 1999), producing a pronounced break in its light curve. As time progresses, it can be observed over wider and wider observing angles, $\theta_{\rm obs}$. Dalal, Griest, & Pruet (2002) have pointed out that as post–jet-break afterglow light curves decay quickly, most orphan afterglows will be dim and hence undetectable. They also suggest that the maximal observing angle $\theta_{\rm max}$ of an orphan afterglow will be a constant factor times θ_j. Hence, the ratio of observed orphan afterglows, $R_{\rm orph}^{\rm obs}$, to that of GRBs, $R_{\rm GRB}^{\rm obs}$, will not tell us much about the opening angles of GRBs and the true rate of GRBs, $R_{\rm GRB}^{\rm true}$.

The observation that GRBs have a constant amount of total energy (Piran et al. 2001; Panaitescu & Kumar 2001; Frail et al. 2001) and that the observed variability in the apparent luminosity arises mostly from variation in the jet opening angles leads to a remarkable result: the post–jet-break afterglow light curve is universal (Granot et al. 2002). We calculate this universal post–jet-break light curve using both first-principle considerations and a calibration from the observed afterglows of GRB 990510 (Harrison et al. 1999; Stanek et al. 1999) and GRB 000926 (Harrison et al.

2001). Using this light curve, we estimate the maximal flux at an observing angle $\theta_{\rm obs}$ from the jet axis. Using this flux, we estimate the total number of orphan afterglows that can be observed given a limiting magnitude and the distribution of these orphan afterglows as a function of $\theta_{\rm obs}$ and the redshift z.

The assumption that the total energy is constant implies that orphan afterglows will be detected roughly up to a constant observing angle $\theta_{\rm max}$ (which is independent of θ_j, for $\theta_j < \theta_{\rm max}$). In this case, $R_{\rm orph}^{\rm obs} \propto R_{\rm GRB}^{\rm true}$ and can teach us about the distribution of θ_j (Granot et al. 2002).

We describe our analytic model and the phenomenological fits to the observations in § 2. We present our estimates for the observed rate of orphan afterglows in § 3. We stress that these are idealized optimistic estimates that do not consider various observational obstacles. We do not consider how and whether these transients could be identified as afterglows and distinguished from other transients. In § 4 we compare our estimates for the expected rate of orphan afterglows with the capabilities of several surveys.

2. THE MODEL

Consider an adiabatic jet with a total energy E and an initial opening angle θ_j. We consider a simple hydrodynamic model for the jet evolution (Rhoads 1999; Sari, Piran, & Halpern 1999). Initially, the jet propagates as if it were spherical, with an equivalent isotropic energy of $2E/\theta_j^2$,

$$E = \frac{2\pi}{3} \theta_j^2 R^3 \gamma^2 n m_p c^2 \, , \tag{1}$$

where n is the ambient number density. The spherical phase continues as long as $\gamma > \theta_j^{-1}$. At this stage, the jet expands

sideways relativistically in the local frame, with $\gamma = \theta^{-1}$, and adiabaticity implies that

$$E = \frac{2\pi}{3} R^3 n m_p c^2 \qquad (2)$$

and that the radius of the shock remains constant.[1] Note that the evolution during this phase is independent of θ_j, whose only role is to determine the time of the jet break. If E and n do not vary from one burst to another, then the light curve during this phase will be universal, depending only on the microscopic parameters (the equipartition parameters $\epsilon_{B,e}$ and the power-law index p of the electron distribution) of the specific afterglow. During both phases, the observed time is given by

$$t = (1+z)\frac{R}{4c\gamma^2} \; . \qquad (3)$$

Equations (2) and (3) yield that the jet-break transition takes place at (Sari et al. 1999)

$$t_{\rm jet} = 0.7(1+z)\left(\frac{E_{51}}{n_0}\right)^{1/3}\left(\frac{\theta_j}{0.1}\right)^2 \; {\rm days} \; , \qquad (4)$$

where Q_x denotes the value of the quantity Q in units of 10^x times its (cgs) units. Due to relativistic beaming, an observer located at $\theta_{\rm obs}$ outside the initial opening angle of the jet ($\theta_{\rm obs} > \theta_j$) will (practically) observe the afterglow emission only at t_θ, when $\gamma = \theta_{\rm obs}^{-1}$:

$$t_\theta = A\left(\frac{\theta_{\rm obs}}{\theta_j}\right)^2 t_{\rm jet} \; . \qquad (5)$$

At around t_θ, the emission is also maximal. From then on it decays in the same way as for an on-axis observer. The factor A in equation (5) is of the order of unity. The value of A is uncertain, and it differs from one model to another. For example, according to model 2 of Granot et al. (2002), $A < 1$ (i.e., the peak flux seen by the observer at $\theta_{\rm obs}$ is seen before the jet opening angle is $\theta_{\rm obs}$), while $A > 1$ according to their model 1. Therefore, lacking better knowledge, we use $A = 1$ throughout this paper.

The synchrotron slow-cooling light curve for the initial (spherical) phase is given by Sari, Piran, & Narayan (1998) and modified by Granot & Sari (2002). Sari et al. (1999) provide temporal scalings for the maximal flux and the synchrotron and cooling frequencies during the modified hydrodynamic evolution after the jet break. Combining both results (using the Granot & Sari 2002 normalization for the fluxes and typical frequencies), we obtain the universal post–jet-break light curve. For the optical band, which is usually above the typical synchrotron frequency but can be either above or below the cooling frequency, we find

$$F_{\nu>\nu_c}(t) = 460\frac{g_0(p)}{g_0(2.2)}10^{(2.2-p)/4}\epsilon_{e,-1}^{p-1}\epsilon_{B,-2}^{(p-2)/4}n_0^{(-p-2)/12}$$
$$\times E_{50.7}^{(p+2)/3}t_{\rm days}^{-p}\nu_{14.7}^{-p/2}(1+z)^{(p+2)/2}D_{L28}^{-2} \; \mu{\rm Jy} \; , \quad (6)$$

$$F_{\nu<\nu_c}(t) = 170\frac{g_1(p)}{g_1(2.2)}10^{(2.2-p)/4}\epsilon_{e,-1}^{p-1}\epsilon_{B,-2}^{(p+1)/4}n_0^{(3-p)/12}E_{50.7}^{(p+3)/3}$$
$$\times t_{\rm days}^{-p}\nu_{14.7}^{(1-p)/2}(1+z)^{(p+3)/2}D_{L28}^{-2} \; \mu{\rm Jy} \; , \qquad (7)$$

---

[1] More detailed calculations show that R increases slowly and γ decreases exponentially with R (Rhoads 1999; Piran 2000).

where D_L is the luminosity distance, $g_0(p) \equiv 10^{-0.56p}(p-0.98)[(p-2)/(p-1)]^{p-1}$, and $g_1(p) \equiv 10^{-0.31p}(p-0.04)[(p-2)/(p-1)]^{p-1}$. The cooling frequency for which equations (6) and (7) give the same flux is

$$\nu_c = 3.62 \times 10^{15}\left(\frac{p-0.98}{p-0.04}\right)^2 10^{(2.2-p)/2}$$
$$\times \epsilon_{B,-2}^{-3/2}n_0^{-5/6}E_{50.7}^{-2/3}(1+z)^{-1} \; {\rm Hz} \; . \qquad (8)$$

Note that ν_c does not depend on θ_j, and it remains constant in time (after the break).

Using equation (5), we obtain the maximal flux that an observer at $\theta_{\rm obs}$ will detect:

$$F_{\nu>\nu_c}^{\rm max}(\theta_{\rm obs}) = 1670\frac{g_0(p)}{g_0(2.2)}A^{-p}\epsilon_{e,-1}^{p-1}\epsilon_{B,-2}^{(p-2)/4}n_0^{(3p-2)/12}$$
$$\times E_{50.7}^{2/3}\nu_{14.7}^{-p/2}(1+z)^{1-p/2}D_{L28}^{-2}\theta_{\rm obs,-1}^{-2p} \; \mu{\rm Jy} \; , \quad (9)$$

$$F_{\nu<\nu_c}^{\rm max}(\theta_{\rm obs}) = 620\frac{g_1(p)}{g_1(2.2)}A^{-p}\epsilon_{e,-1}^{p-1}\epsilon_{B,-2}^{(p+1)/4}n_0^{(p+1)/4}$$
$$\times E_{50.7}\nu_{14.7}^{(1-p)/2}(1+z)^{(3-p)/2}$$
$$\times D_{L28}^{-2}\theta_{\rm obs,-1}^{-2p} \; \mu{\rm Jy} \; . \qquad (10)$$

One notices here a very strong dependence on $\theta_{\rm obs}$. The peak flux drops quickly when the observer moves away from the axis. Note also that this maximal flux is independent of the opening angle of the jet θ_j.

Once we know $F_\nu^{\rm max}(\theta_{\rm obs})$, we can estimate $\theta_{\rm max}(z, m)$, the maximal observing angle at which an afterglow is brighter than a limiting magnitude m. We then proceed and estimate the total number of orphan afterglows brighter than m.

We can estimate the observed flux using the "canonical" values of the parameters. However, these are uncertain. Alternatively, we can use the observations of the afterglows of GRB 990510 (Harrison et al. 1999; Stanek et al. 1999) and GRB 000926 (Harrison et al. 2001), both showing clear jet breaks, to obtain an "observational" calibration of $F_\nu(\theta_{\rm obs})$. As the $\theta_{\rm obs}$ dependence in equations (9) and (10) is similar, we can write

$$F(\theta_{\rm obs}) = F_0 f(z)\theta_{\rm obs}^{-2p} \; , \qquad (11)$$

where F_0 is a constant and $f(z) = (1+z)^{1+\beta}D_{L28}^{-2}$ includes all the cosmological effects. The quantity β is the spectral slope ($F_\nu \propto \nu^\beta$). The value of β depends on whether the observed frequency is below or above the cooling frequency ν_c: $\beta_{\nu<\nu_c} = (1-p)/2$ and $\beta_{\nu>\nu_c} = -p/2$. For simplicity, we consider throughout the paper only the case where $\nu > \nu_c$ and $\beta = -p/2$.

If all GRBs are similar with the same total energy, ambient density, and microscopic parameters ($\epsilon_{e,B}$ and p), then F_0 is a "universal" constant. However, its value is uncertain. We need the observed flux and θ at a certain time to determine F_0. We use the on-axis observed afterglows at the break time, when an observer at $\theta_{\rm obs} = \theta_j A^{-1/2}$ (for a narrower jet) would observe a flux similar to that seen by an on-axis observer (for the observed jet). Using the parameters for GRB 990510 and GRB 000926, we estimate F_0 directly. For GRB 990510 (Harrison et al. 1999), we have $\theta_j = 0.08$, $p = 2.1$, $z = 1.6$, and $m_{\rm break} = 20$ mag, where $m_{\rm break}$ is the R-band magnitude of the afterglow at the break time and $F_0(990510) = 0.01$ μJy. For GRB 000926 (Harrison et al.

2001), $\theta_j = 0.1$, $p = 2.2$, $z = 2$, $m_{break} = 20$ mag, and $F_0(000926) = 0.03$ μJy. Both values are rather close to the theoretical estimate with $E_{51} = 0.5$, $n = 1$, $\epsilon_e = 0.1$, $\epsilon_B = 0.01$, and $p = 2.2$, which yields $F_0 = 0.02$ μJy and magnitude 20 at the break time (for a burst at $z = 2$ with $\theta_j = 0.1$).

Using a more refined simulation of the off-axis light curve (their model 2), Granot et al. (2002) show that when the off-axis light curve "joins" the on-axis light curve, the off-axis maximal flux is a factor of a few less than the on-axis flux. For example, a burst at $z = 1$ with $E_{51} = 0.5$, $n = 1$, $\epsilon_e = 0.1$, $\epsilon_B = 0.01$, and $p = 2.5$ is estimated in this model to be 24th magnitude at $\theta_{obs} = 0.22$. This result corresponds to $F_0 = 0.002$ μJy. According to the observations and the fact that the off-axis maximal flux is a factor of a few less than the on-axis flux, we use in the following a "canonical" model of $F_0 = 0.003$ μJy and $p = 2.2$. We should keep in mind that there is a large uncertainty (factor of $\sim$10) in the absolute value of the flux. This uncertainty does not change θ_{max}, which scales as $F_0^{1/2p}$, by a large factor. However, the overall detection rate depends almost linearly on F_0. The total number of observed bursts depends not only on $\theta_{max}^2 \propto F_0^{1/p}$, but also on the duration t_{obs} (see eq. [12] below), which is $\propto\theta_{max}^2$. With both of these together, we find that the rate is $\propto F_0^{2/p}$.

For a given limiting magnitude m, we can now calculate the total number of observed orphan afterglows. For a given z, we define $\theta_{max}(z, m)$ such that $23.6 - 2.5\log_{10}$

$\{F_\nu[\theta_{max}(z, m)]\} = m$, where F_ν is the observed flux in units of μJy. Figure 1 depicts contour lines of the inverse function $m(\theta_{obs}, z)$ on the (θ_{obs}, z)-plane. We use throughout this paper a "standard" cosmological model with $\Omega_M = 0.3$, $\Omega_\Lambda = 0.7$, and $h = 0.7$.

According to our model, an observer at θ_{obs} will observe the orphan afterglow if $\theta_{obs} < \theta_{max}(z, m)$. The afterglow will be detectable over a time

$$t_{obs}(z, \theta, m) \approx \frac{At_{jet}}{\theta_j^2}\left(\theta_{max}^2 - \theta_{obs}^2\right), \qquad (12)$$

until the signal decays below the limiting magnitude. In this model, which we denote model A, an orphan afterglow could be observed from a solid angle[2] $2\pi[\theta_{max}(z, m)^2 - \theta_j^2]$, where $\theta_{max}(z, m)$ does not depend on θ_j. This model, and more specifically equation (11), are quite generally valid for $\theta_{max} > \theta_j$. However, if $\theta_{obs} \sim \theta_j$, $F_\nu^{max}(\theta_{obs})$ is more sensitive to the exact jet model being used. Specifically, in such a case there will be significant contributions to the signal at θ_{obs}, even before the jet's opening angle reaches θ_{obs}. This leads to a larger flux at θ_{obs} and hence to a larger θ_{max}. For example, Granot et al. (2002) find for their model 2 that the solid angle between θ_j and the real maximal angle ($\tilde{\theta}_{max}$) is approximately constant, even when θ_{obs} exceeds the asymp-

---

[2] The factor of 2 reflects the expectation that the jets are double sided.
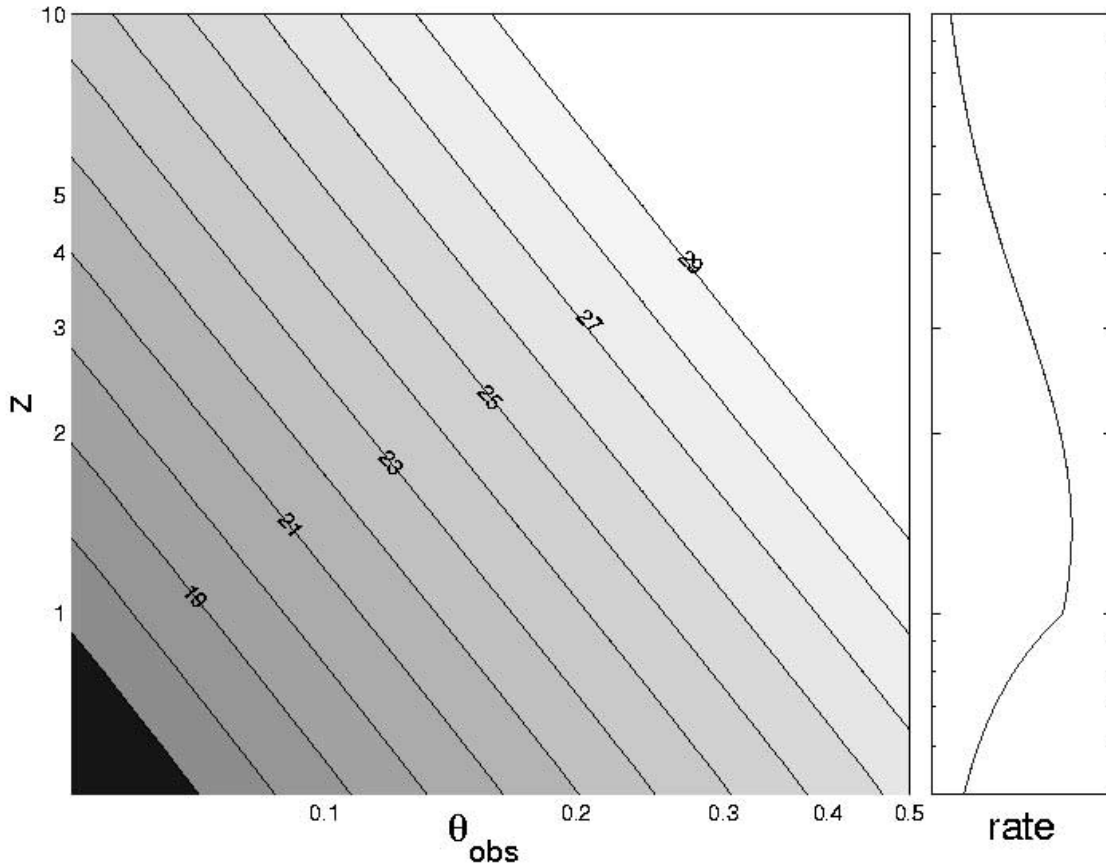

Fig. 1.—*Left*: R-magnitude contour lines (from 17 at bottom left to 29) for $F_0 = 0.003$ μJy. *Right*: GRB rate $n(z)(dV/dz)/(1 + z)$ as a function of z (for $z_{peak} = 1$), as an indication to where we should expect most GRBs. As we plot only the region with $z > 0.5$, the flux depends almost as a power law on the redshift. [*See the electronic edition of the Journal for a color version of this figure*.]

totic value of $\theta_{\max}$ (given by eq. [11]), i.e., $\tilde{\theta}_{\max}^2 = \theta_{\max}^2 + \theta_j^2$. To take care of this effect, we also consider model B, in which we assume that this relation holds. While model A is more conservative, model B allows for more orphan afterglows. We see later that for $m_{\lim} \geq 25$ surveys, both models give comparable results. Model B gives a factor of 2.5 more orphan afterglows for $m_{\lim} = 23$ (with our "canonical" parameters). It also predicts a larger ratio of orphan-to–on-axis afterglows.

3. RESULTS

The rate of observed orphan afterglows (over the entire sky) is (in model A)

$$R_{\text{orph}} = \int_0^{10} \frac{n(z)}{(1+z)} \frac{dV(z)}{dz} dz \int_{\theta_j}^{\theta_{\max}(z,\,m)} \theta \, d\theta , \quad (13)$$

where $n(z)$ is the rate of GRBs per unit volume and unit proper time and $dV(z)$ is the differential volume element at redshift z. We assume that the GRB rate is proportional to the star formation rate (SFR) and is given by $n(z) = B10^{0.75z}$ for $z \leq z_{\text{peak}}$ and $n(z) = B10^{0.75z_{\text{peak}}}$ for $z_{\text{peak}} < z < 10$. The normalization factor B is found by the condition $R_{\text{GRB}}^{\text{true}} = f_b R_{\text{GRB}}^{\text{obs}} = \int_0^{10} (dV/dz)[n(z)/(1+z)] dz$, where f_b is the beaming factor and $R_{\text{GRB}}^{\text{obs}} = 667 \text{ yr}^{-1}$. In the following, we consider two SFRs peaking at $z_{\text{peak}} = 1$ and 2 (Bouwenn, Broadhurst, & Illingworth 2002).

Usually, the detector's exposure time is smaller than $t_{\text{obs}}(z, \theta, m)$. Thus, the number of detectable orphan afterglows in a single snapshot over the whole sky is

$$N_{\text{orph}} = \int_0^{10} \frac{n(z)}{(1+z)} \frac{dV(z)}{dz} dz$$
$$\times \int_{\theta_j}^{\theta_{\max}(z,m)} t_{\text{obs}}(z, \theta, m)\theta \, d\theta . \quad (14)$$

If we now consider model B, we find

$$R_{\text{orph}}^{(B)} = \frac{1}{2} \left(\frac{F_0}{F_{\lim}} \right)^{1/p} \int_0^{10} \frac{n(z)}{(1+z)} \frac{dV(z)}{dz} f(z)^{1/p} dz, \quad (15)$$

where $F_{\lim}$ is the limiting flux for detection. In this case, $R_{\text{orph}}/R_{\text{GRB}}^{\text{true}} \sim (F_0/F_{\lim})^{1/p}$ is independent of f_b. Using $t_{\text{obs}}(\theta_{\text{obs}}) \approx t_\theta(\theta_{\max}) - t_\theta(\theta_{\text{obs}})$, we estimate the number of observed orphan afterglows:

$$N_{\text{orph}}^{(B)} = \frac{At_{\text{jet}}}{4(1+z)\theta_j^2} \left(\frac{F_0}{F_{\lim}} \right)^{2/p}$$
$$\times \int_0^{10} n(z) \frac{dV(z)}{dz} f(z)^{2/p} dz . \quad (16)$$

We note that since $F_0 \propto A^{-p}$, both $R_{\text{orph}}^{(B)}$ and $N_{\text{orph}}^{(B)}$ scale as $1/A$.

The z integrand of equation (14) gives the normalized redshift distribution of the observed orphan afterglows for model A (see Fig. 2a). This distribution has a broad flat region all the way from $z \approx 0$ to z_{peak}. It sharply declines above z_{peak}. For an SFR with a higher z_{peak}, there are significantly fewer orphan afterglows (see Fig. 3). The function peaks (weakly) at z_{peak} with a higher limiting magnitude, as more orphan afterglows are observed in this case. For model B, the results are similar.
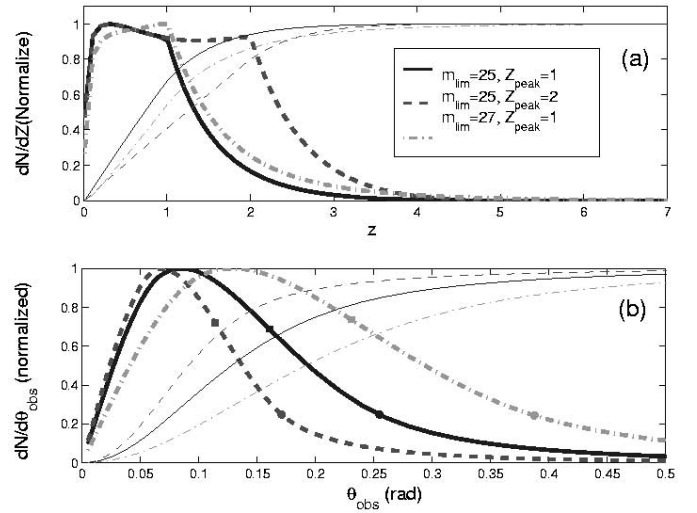

Fig. 2.—(a) Normalized redshift distribution of observed orphan afterglows in a single snapshot (*thick lines*) and the integrated z distribution (*thin lines*). (b) Angular distribution of observed orphan afterglows in a single snapshot (*thick lines*) and the integrated θ_{obs} distribution (*thin lines*). The circles depict $\theta_{\max}(z_{\text{peak}}, m)$ and the squares depict $\langle \theta_{\text{obs}} \rangle$. In both panels, we use $F_0 = 0.003 \, \mu$Jy and $\theta_j = 0.1$. The different curves correspond to $m_{\lim} = 25$, $z_{\text{peak}} = 1$ (*solid line*); $m_{\lim} = 25$, $z_{\text{peak}} = 2$ (*dashed line*); $m_{\lim} = 27$, $z_{\text{peak}} = 1$ (*dot-dashed line*); and $m_{\lim} = 27$, $z_{\text{peak}} = 2$ (*dotted line*). [*See the electronic edition of the Journal for a color version of this figure.*]

The θ integrand of equation (14) [with $\theta_{\max}(z, m)$ replaced by $z_{\max}(\theta, m)$ and integration performed over z] yields the angular distribution for model A (see Fig. 2b). For a 25th limiting magnitude, the median observing angle will be $5°$–$7°$, depending on the SFR. With a lower z_{peak},
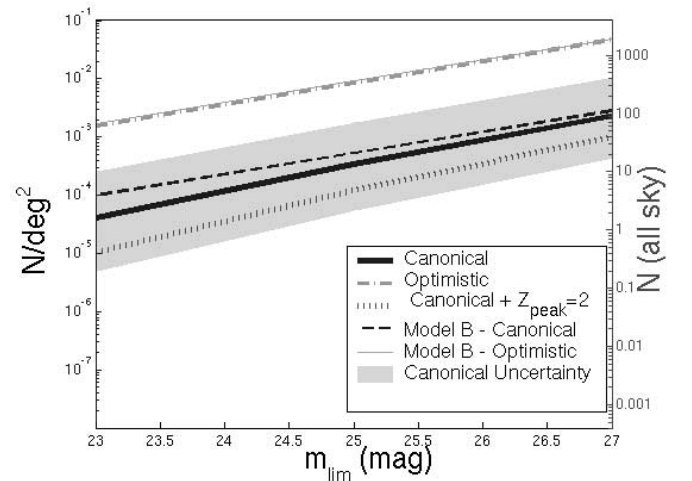

Fig. 3.—Number of observed orphan afterglows per square degree (*left vertical scale*) and in the entire sky (*right vertical scale*), in a single exposure, as a function of the limiting magnitude for detection. The thick lines are for model A with three different sets of parameters: (1) Our "canonical" normalization $F_0 = 0.003 \, \mu$Jy, $z_{\text{peak}} = 1$, and $\theta_j = 0.1$ (*solid line*). The gray area around this line corresponds an uncertainty by a factor of 5 in this normalization. (2) Our most optimistic model with a relatively small $\theta_j = 0.05$ and a large $F_0 = 0.015 \, \mu$Jy (*dot-dashed line*). (3) The same as our "canonical" model, except for $z_{\text{peak}} = 2$ (*dotted line*). The thin lines are for model B, where the solid line is for our "optimistic" parameters, while the dashed line is for our "canonical" parameters. Both models are similar for the "optimistic" parameters, while model B predicts slightly more orphan afterglows than model A for the "canonical" parameters. [*See the electronic edition of the Journal for a color version of this figure.*]

TABLE 1
The Ratio of the Number of Orphan Afterglows to the Total Number of Afterglows
(Both On-Axis and Orphan) in a Single Snapshot

		Ratio					
		$m_{\lim} = 23$		$m_{\lim} = 25$		$m_{\lim} = 27$	
$z_{\rm peak}$	θ_j	Model A	Model B	Model A	Model B	Model A	Model B
1........	0.05	0.76	0.81	0.88	0.90	0.95	0.95
	0.10	0.4	0.63	0.64	0.73	0.81	0.84
	0.15	0.2	0.55	0.4	0.63	0.64	0.74
2........	0.10	0.2	0.56	0.44	0.64	0.69	0.76

most GRBs will be nearer and hence stronger and detectable to slightly larger angles. These values will be close to the jet opening angles. Most of the observed orphan afterglows with this limiting magnitude will be " near misses " of on-axis events. The $\theta_{\max}(z_{\rm peak})$ will be significantly larger ($10°$–$14°$). At 27th magnitude, the median of the angular distribution moves way out to $12°$. This is larger than most GRB beaming angles, but still narrow, corresponding to only 2% of the sky. Again, the results for model B are similar (as long as $\theta_j \lesssim 0.1$).

As the sky coverage of GRB detectors is not a continuous 4π, it is possible that a GRB pointing toward us (i.e., with $\theta_{\rm obs} < \theta_j$) will be missed, but its on-axis afterglow will be detected. In Table 1 we provide the ratio of the number of orphan afterglows to the total number of afterglows (both on-axis and orphan) in a single snapshot of the sky. As expected, this ratio is large for small jet opening angles and for large limiting magnitudes (and models A and B give similar results in this limit), and it decreases with increasing θ_j and decreasing $m_{\lim}$. An insensitive search ($m_{\lim} = 23$) yields for model A a comparable (or even larger) probability that a visual transient is a missed on-axis GRB whose afterglow is detected as opposed to an orphan afterglow. However, for model B, this ratio is less sensitive to either θ_j or $m_{\lim}$ for $\theta_j \sim \theta_{\max}$, and even for $m_{\lim} = 23$, the majority of the afterglows would be orphans.

Figure 3 depicts the number of orphan afterglows per square degree (and in the entire sky), in a single exposure, as a function of the limiting magnitude. The thick lines are for model A (with various parameters), while the thin lines are for model B. In the " optimistic " case ($F_0 = 0.015$ μJy, $\theta_j = 0.05$), the predictions of both models are similar. With the " canonical " normalization ($F_0 = 0.003$ μJy, $z_{\rm peak} = 1$, and $\theta_j = 0.1$), model B predicts 2.5 times more orphan afterglows than model A, for a limiting magnitude of 23. These numbers provide an upper limit to the rate at which orphan afterglows will be recorded as pointlike optical transients in any exposure with a given limiting magnitude. These numbers should be considered as upper limits, as our estimates do not include effects such as dust extinction that could make these transients undetectable.

We ask now: What will be the optimal strategy for a given observational facility, short and shallow exposures that cover a larger solid angle or long and deep ones over a smaller area? The exposure time that is required in order to reach a given limiting flux $F_{\lim}$ is proportional to $F_{\lim}^{-2}$. We can now divide the number density of observed orphan afterglows (shown in Fig. 3) by this time factor and obtain the rate per square degree per hour for an observational

facility. Figure 4 depicts this rate with a calibration to a hypothetical 2 m class telescope that reaches the 25th magnitude with a 1 hr exposure. Other telescopes will have another normalization, but the trend seen in this figure remains. Figure 4 shows that shallow surveys that cover a large area are preferred over deep ones (in both models). This result can be understood as follows: Multiplying equation (16) by $F_{\lim}^2$ shows that the rate per square degree per hour of observational facility $\propto F_{\lim}^{2-2/p}$. As $p > 1$ ($2 - 2/p > 0$), a shallow survey is preferred. A practical advantage of this strategy is that it would be easier to carry out follow-up observations with a large telescope on a brighter transient detected in a shallow survey. In addition, one can expect that the number of spurious transients will be smaller in a shallower survey. However, if one wishes to detect orphan afterglows, one should still keep the surveys at a limiting magnitude of ~ 23, since for smaller magnitudes, the number of on-axis transients detected will be comparable to (model B) or even larger than (model A) the number of orphan afterglows (see Table 1).

The number density of orphan afterglow transients, given by equation (14) or (16) and depicted in Figure 3, gives an
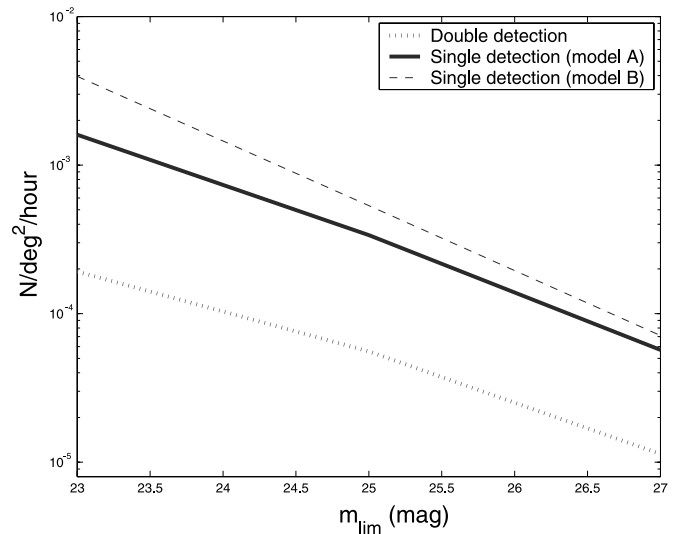

Fig. 4.—Detection rate of orphan afterglows per square degree per hour of telescope time. The curves that correspond to the " canonical " normalization are for a single detection in model A (*solid line*), a single detection in model B (*dashed line*), and a double detection in model A (*dotted line*). The rate is calibrated for a telescope that reaches $m_{\lim} = 25$ in a 1 hr exposure. It can be scaled up or down for other telescopes. [*See the electronic edition of the Journal for a color version of this figure.*]

indication of the number of single events recorded above a limiting magnitude. Clearly, a single detection is not enough in order to identify that the transient indeed corresponds to an afterglow. A second following detection of the transient with a decrease by, for instance, 1 mag, would increase the probability that the transient is an orphan afterglow. We estimate the rate of a double detection of this nature by an afterglow search with a limiting magnitude m_{lim} and a time delay dT_{obs} between two exposures of the same region in the sky. We consider, therefore, a detection of a transient in one exposure and a second detection after time dT_{obs} in which the transient has decayed by more than 1 mag but is still above the limiting magnitude of the survey. This is of course an idealized situation, and we do not consider realistic observational problems (such as weather, etc.) that may make the detection rate lower. Not surprisingly, the ratio of a double detection to a single detection depends on the time delay, dT_{obs} (see Fig. 5). The optimal time delay is the time in which an afterglow from z_{peak} and with $m_{lim} - 1$ decays by 1 mag: $dT_{obs} = 3$ days for $m_{lim} = 23$, $dT_{obs} = 4$ days for $m_{lim} = 25$, and $dT_{obs} = 8$ days for $m_{lim} = 27$. With this optimal choice, the fraction of the detected transients that will be detected in a second exposure is 20% for $m_{lim} = 27$ and 12% for $m_{lim} = 23$. Note, however, that the curve becomes narrower for low limiting magnitudes, making the exact timing of the second exposure more critical. Deeper surveys are less sensitive to the choice of the time delay.

It is interesting to compare the rate of observed orphan afterglows with the true GRB rate as a function of the beaming factor, $f_b \approx 2/\theta_j^2$. At this point, models A and B differ the most. For model B, this ratio is $\propto (F_0/F_{lim})^{1/p}$, and for the "canonical" parameters, it holds the values of 0.004, 0.014, and 0.031 for $m_{lim} = 23$, 25, and 27, independently of f_b. In model A, this ratio vanishes for low f_b-values. For high f_b-values, the ratio converges to the model B constant ratio. For the "canonical" parameters, this ratio in model A reaches half of the asymptotic value for $f_b > 50$, 125, and 250 for $m_{lim} = 27$, 25, and 23, respectively. Thus, for strong

beaming (or high m_{lim}), it is possible to estimate the true GRB rate from a determination of the orphan afterglow rate. For a low beaming factor, this ratio is model dependent.

4. DISCUSSION

We have calculated the number per unit solid angle of orphan afterglows that could be detected by idealized surveys with different limiting magnitudes. Our calculations are based on a simple idealized model for the hydrodynamics of the sideways expanding jets. Light curves from other models, including numerical simulations (Granot et al. 2001) described in Granot et al. (2002), show similar behavior. As the models differ when $\theta_{obs} \sim \theta_j$, we also consider an alternative assumption for this range. This yields analytic expressions for R_{orph} and N_{orph} (eqs. [15] and [16]). We have shown that both models yield similar results for surveys deeper than $m_{lim} = 25$ and have minor differences for surveys with $m_{lim} \sim 23$.

The normalization factor F_0 of this light curve (eq. [11]) is somewhat sensitive to the choice of model parameters. Even observed afterglows with a clear jet break do not yield a well-defined normalization factor, $F_0 = A^{-p}f(z)^{-1}\theta_j^{2p} F_\nu(t_{jet}, \theta_{obs} = 0)$, because of the uncertainties in θ_j, A, and $F_\nu(t_{jet}, \theta_{obs} = 0)$. As $N_{orph} \propto AF_0^{2/p} \propto F_\nu(t_{jet}, \theta_{obs} = 0)^{2/p}/A$ (eq. [16]), we expect the uncertainty in N_{orph} to be similar to that in F_0 (a factor of ~ 10). However, this uncertainty does not influence the trends that indicate a strategy for an optimal orphan afterglow survey.

We stress that we do not consider here practical observational issues, such as dust extinction or the ability to identify a weak transient on top of a background host galaxy. We have also assumed idealized weather conditions: when considering a "verified" identification by two successive detections, we assumed that a second exposure is always possible. All these factors will reduce the observed rate by some unknown factors below our optimistic values. We do not consider how recorded transients could be identified as afterglows. For example, when we discuss a single detection, we mean a single photometric record of a transient in a single snapshot. This is of course a very weak requirement, and much more (at least a second detection) would be needed to identify this event as an afterglow.

Finally, one should be aware of the possible confusion between orphan afterglows and other transients. Most transients could be completely unrelated (such as supernovae or active galactic nuclei [AGNs]) and could be distinguished from afterglows with follow-up observations. However, there could be a class of related transients such as on-axis jets whose gamma-ray emission was not observed because of lack of coverage or failed GRBs (Huang, Dai, & Lu 2002). The only quantitative measure that we provide is for the ratio of on-axis afterglows to truly orphan ones (i.e., off-axis afterglows whose prompt gamma-ray emission would have been detectable if viewed from within the jet opening angle).

We have shown that for a given dedicated facility, the optimal survey strategy will be to perform many shallow snapshots. However, those should not be too shallow, as we will observe more on-axis afterglows than off-axis ones. A reasonable limiting magnitude will be $\sim 23-25$. With this magnitude, we should perform a repeated snapshot of the same region after 3–4 days.
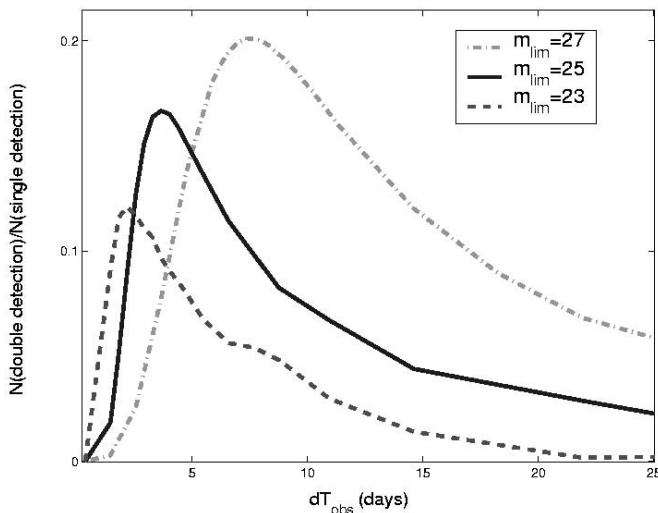

FIG. 5.—Ratio of double detection of orphan afterglows to a single detection, as a function of the time delay dT_{obs} between the two exposures. The three models are $F_0 = 0.003$ μJy, $z_{peak} = 1$, and $m_{lim} = 23$ (*dashed line*), 25 (*solid line*), and 27 (*dot-dashed line*). [*See the electronic edition of the Journal for a color version of this figure.*]

We consider now several possible surveys. The Sloan Digital Sky Survey (SDSS; York et al. 2000) has $m_{lim} \sim 23$ over 10^4 deg^2 in the north Galactic cap. Figure 3 suggests that under the most optimistic conditions, we expect 15 detections of orphan afterglow transients in the north Galactic cap of the SDSS. A careful comparison of the SDSS sky coverage and the exposure of relevant GRB satellites could reveal the rate of coincident detection (GRB-Sloan optical transient), from which one could get a better handle (using Table 1) on the possible rate of detection of orphan afterglows by SDSS. Under more realistic assumptions, we expect a single orphan afterglow transient in the SDSS. Note that the five-filter SDSS system could even possibly select orphan afterglow candidates with only a single detection (Rhoads 2001; Vanden Berk et al. 2002), although this method could only be applied to bright sources. As the north Galactic cap survey provides only a single snapshot with no spectral information at a magnitude of 23, even if a transient were recorded in this survey, it would be impossible to identify it as a transient. Clearly, this is not the best survey for an orphan afterglow search. However, the south Galactic cap survey observes the same part of the sky repeatedly with $m_{lim} \sim 23$. It can achieve a higher magnitude (25th) for steady sources. If the repetition interval is longer than 2 weeks, than for most orphan afterglows, the second observation can be considered as a new one. Therefore, given that the time spent in the south cap is comparable to the time spent in the north cap, the detection rate should be comparable. The advantage of the south cap is the ability to identify transient sources, even if the decay process cannot be observed, and the possibility of ruling out sources that are not transient in nature, such as AGNs.

Consider now a dedicated 2 m class telescope with an aperture of 0.5 deg^2, with $m_{lim} = 24$ for a 10 minute exposure and $m_{lim} = 25$ for a 1 hr exposure. Under our most optimistic assumptions, it will record up to 35 orphan afterglows per year in the shallow mode and a third of that (13 afterglows) in the deeper mode. Using our "canonical" model, we find two orphan afterglows per year in the shallow mode.

The VIMOS camera at the Very Large Telescope has a comparable aperture of 0.06 deg^2, but it can reach $m_{lim} = 26$ in 10 minutes and $m_{lim} = 27$ in 1 hr. A single $m_{lim} = 27$ frame would have 0.002 orphan afterglows under the most optimistic assumptions (1.1×10^{-4}, canonically). Thus, at best 2–3 orphan afterglows should be hiding in every 1000 exposures. The Subaru Suprime-Cam has a similar sensitivity, but its field of view is 4 times larger. Therefore, every 1000 exposures should contain no more than 10 orphan afterglows. It will be, however, a remarkable challenge to pick up these transients and confirm their nature from all other data gathered in these 1000 exposures.

REFERENCES

Bouwenn, E. N. S., Broadhurst, T. J., & Illingworth, R. J. 2002, ApJ, submitted
Dalal, N., Griest, K., & Pruet, J. 2002, ApJ, 564, 209
Frail, D. A., et al. 2001, ApJ, 562, L55
Granot, J., Miller, M., Piran, T., Suen, W. M., & Hughes, P. A. 2001, in Gamma-Ray Bursts in the Afterglow Era, ed. E. Costa, F. Frontera, & J. Hjorth (Berlin: Springer), 312
Granot, J., Panaitescu, A., Kumar, P., & Woosley, S. E. 2002, ApJ, 570, L61
Granot, J., & Sari, R. 2002, ApJ, 568, 820
Harrison, F. A., et al. 1999, ApJ, 523, L121
———. 2001, ApJ, 559, 123
Huang, Y. F., Dai, Z. G., & Lu, T. 2002, MNRAS, 332, 735
Panaitescu, A., & Kumar, P. 2001, ApJ, 560, L49

Piran, T. 1994, in AIP Conf. Proc. 307, Gamma-Ray Bursts, ed. G. J. Fishman, J. J. Brainerd, & K. Hurley (New York: AIP), 495
———. 2000, Phys. Rep., 333, 529
Piran, T., Kumar, P., Panaitescu, A., & Piro, L. 2001, ApJ, 560, L167
Rhoads, J. E. 1997, ApJ, 487, L1
———. 1999, ApJ, 525, 737
———. 2001, ApJ, 557, 943
Sari, R., Piran, T., & Halpern, J. P. 1999, ApJ, 519, L17
Sari, R., Piran, T., & Narayan, R. 1998, ApJ, 497, L17
Stanek, K. Z., Garnavich, P. M., Kaluzny, J., Pych, W., & Thompson, I. 1999, ApJ, 522, L39
Vanden Berk, D., et al. 2002, ApJ, 576, 673
York, D. G., et al. 2000, AJ, 120, 1579